Applications of random matrix theory for sensor array imaging with measurement noise

Josselin Garnier* Knut Sølna†

June 17, 2014

Abstract

The imaging of a small reflector embedded in a medium is a central problem in sensor array imaging. The goal is to find a reflector embedded in a medium. The medium is probed by an array of sources, and the signals backscattered by the reflector are recorded by an array of receivers. The responses between all pairs of source and receiver are collected so that the available information takes the form of a response matrix. When the data are corrupted by additive measurement noise we show how tools of random matrix theory can help to detect, localize, and characterize the reflector.

AMS subject classifications. Primary 78A46; Secondary 15B52.

1 Introduction

The imaging of a small reflector embedded in a medium is a central problem in wave sensor imaging [6, 26]. Sensor array imaging involves two steps. The first step is experimental, it consists in emitting waves from an array of sources and recording the backscattered signals by an array of receivers. The data set then consists of a matrix of recorded signals whose indices are the index of the source and the index of the receiver. The second step is numerical, it consists in processing the recorded data in order to estimate the quantities of interest in the medium (reflector locations,...). The main applications of sensor array imaging are medical imaging, geophysical exploration, and non-destructive testing.

Recently it has been shown that random matrix theory could be used in order to build a detection test based on the statistical properties of the singular values of the response matrix [7, 8, 9, 1, 2]. This paper summarizes the results contained in [1, 2] and extends them into several important directions. First we address in this paper the case in which the source array and the receiver array are not coincident, and more generally the case in which the number of sources is different from the number of receivers. As a result the noise singular value distribution has the form of a deformed quarter circle and the statistics of the singular value associated to the reflector is also affected. Second we study carefully the estimation of the noise variance of the response matrix. Different estimators are studied and an estimator that achieves an efficient trade-off between bias and variance is proposed. The use of this estimator instead of the empirical estimator used in the previous versions significantly improves the quality of the detection test based on the singular value distribution of the measured response matrix when the number of sensors is not very large. Third we propose an algorithm that can reconstruct not only the position of the reflector, but also its scattering amplitude. The estimator of the scattering amplitude compensates for the level repulsion of the singular value associated to the reflector due to the noise.

*Laboratoire de Probabilités et Modèles Aléatoires & Laboratoire Jacques-Louis Lions, Université Paris VII, 75205 Paris Cedex 13, France (garnier@math.univ-paris-diderot.fr)

†Department of Mathematics, Universite of California at Irvine, Irvine, CA 92697 (ksolna@math.uci.edu).

2 The Response Matrix

We address the case of a reflector that can model a small dielectric anomaly in electromagnetism, a small density anomaly in acoustics, or more generally a local variation of the index of refraction in the scalar wave equation. We consider the case in which the contrast of the anomaly (its index of refraction relative to the one of the background medium) can be of order one but its diameter is assumed to be small compared to the wavelength. In such a situation it is possible to expand the solution of the wave equation around the background solution, as we explain below [3, 4, 5].

Let us consider the scalar wave equation in a d-dimensional homogeneous medium with the index of refraction n_0. The reference speed of propagation is denoted by c. The index of refraction of the reflector or inclusion D is $n_{\rm ref} \neq n_0$. The support of the inclusion is of the form $D = \boldsymbol{x}_{\rm ref} + B$, where B is a domain with small volume and $\boldsymbol{x}_{\rm ref}$ is the location of the reflector. Therefore the scalar wave equation with the source $S(t, \boldsymbol{x})$ takes the form

$$\frac{n^2(\boldsymbol{x})}{c^2}\partial_t^2 E - \Delta_{\boldsymbol{x}} E = S(t, \boldsymbol{x}),$$

where the index of refraction is given by

$$n(\boldsymbol{x}) = n_0 + (n_{\rm ref} - n_0)\mathbf{1}_D(\boldsymbol{x}).$$

In this paper we consider time-harmonic point sources emitting at frequency ω. For any $\boldsymbol{y}_n, \boldsymbol{z}_m$ far from $\boldsymbol{x}_{\rm ref}$ the field $\mathrm{Re}(\hat{E}(\boldsymbol{y}_n, \boldsymbol{z}_m)e^{-i\omega t})$ observed at $\boldsymbol{y}_n$ when a point source emits a time-harmonic signal with frequency ω at $\boldsymbol{z}_m$ can be expanded as powers of the volume of the inclusion as

$$\hat{E}(\boldsymbol{y}_n, \boldsymbol{z}_m) = \hat{G}(\boldsymbol{y}_n, \boldsymbol{z}_m) + k_0^2 \rho_{\rm ref} \hat{G}(\boldsymbol{y}_n, \boldsymbol{x}_{\rm ref})\hat{G}(\boldsymbol{x}_{\rm ref}, \boldsymbol{z}_m) + O(|B|^{\frac{d+1}{d}}), \tag{1}$$

where $k_0 = n_0\omega/c$ is the homogeneous wavenumber, $\rho_{\rm ref}$ is the scattering amplitude

$$\rho_{\rm ref} = \Big(\frac{n_{\rm ref}^2}{n_0^2} - 1\Big)|B|, \tag{2}$$

and $\hat{G}(\boldsymbol{x}, \boldsymbol{z})$ is the Green's function or fundamental solution of the Helmholtz equation with a point source at $\boldsymbol{z}$:

$$\Delta_{\boldsymbol{x}}\hat{G}(\boldsymbol{x}, \boldsymbol{z}) + k_0^2\hat{G}(\boldsymbol{x}, \boldsymbol{z}) = -\delta(\boldsymbol{x} - \boldsymbol{z}). \tag{3}$$

More explicitly we have

$$\hat{G}(\boldsymbol{x}, \boldsymbol{z}) = \begin{cases} \dfrac{i}{4}H_0^{(1)}(k_0|\boldsymbol{x} - \boldsymbol{z}|) & \text{if } d = 2, \\ \dfrac{e^{ik_0|\boldsymbol{x}-\boldsymbol{z}|}}{4\pi|\boldsymbol{x} - \boldsymbol{z}|} & \text{if } d = 3, \end{cases}$$

where $H_0^{(1)}$ is the Hankel function of the first kind of order zero.

When there are M sources $(\boldsymbol{z}_m)_{m=1,\dots,M}$ and N receivers $(\boldsymbol{y}_n)_{n=1,\dots,N}$, the response matrix is the $N \times M$ matrix $\mathbf{A}_0 = (A_{0nm})_{n=1,\dots,N,m=1,\dots,M}$ defined by

$$A_{0nm} := \hat{E}(\boldsymbol{y}_n, \boldsymbol{z}_m) - \hat{G}(\boldsymbol{y}_n, \boldsymbol{z}_m). \tag{4}$$

This matrix has rank one:

$$\mathbf{A}_0 = \sigma_{\rm ref}\boldsymbol{u}_{\rm ref}\boldsymbol{v}_{\rm ref}^\dagger, \tag{5}$$

where $\dagger$ stands for the conjugate transpose. The unique nonzero singular value of this matrix is

$$\sigma_{\rm ref} = k_0^2\rho_{\rm ref}\Big(\sum_{l=1}^N |\hat{G}(\boldsymbol{y}_l, \boldsymbol{x})|^2\Big)^{1/2}\Big(\sum_{l=1}^M |\hat{G}(\boldsymbol{z}_l, \boldsymbol{x})|^2\Big)^{1/2}. \tag{6}$$

The associated left and right singular vectors $\boldsymbol{u}_{\rm ref}$ and $\boldsymbol{v}_{\rm ref}$ are given by:

$$\boldsymbol{u}_{\rm ref} = \boldsymbol{u}(\boldsymbol{x}_{\rm ref}), \qquad \boldsymbol{v}_{\rm ref} = \boldsymbol{v}(\boldsymbol{x}_{\rm ref}), \tag{7}$$

where we have defined the normalized vectors of Green's functions:

$$\boldsymbol{u}(\boldsymbol{x}) = \Big(\frac{\hat{G}(\boldsymbol{y}_n, \boldsymbol{x})}{\big(\sum_{l=1}^N |\hat{G}(\boldsymbol{y}_l, \boldsymbol{x})|^2 \big)^{1/2}} \Big)_{n=1,\ldots,N}, \qquad \boldsymbol{v}(\boldsymbol{x}) = \Big(\frac{\overline{\hat{G}(\boldsymbol{z}_m, \boldsymbol{x})}}{\big(\sum_{l=1}^M |\hat{G}(\boldsymbol{z}_l, \boldsymbol{x})|^2 \big)^{1/2}} \Big)_{m=1,\ldots,M}. \tag{8}$$

The matrix $\mathbf{A}_0$ is the complete data set that can be collected. In practice the measured matrix is corrupted by electronic or measurement noise that has the form of an additive noise, with uncorrelated entries. The purpose of this paper is to address the classical imaging problems given the measured data set:
- is there a reflector in the medium ? This is the detection problem. In the absence of noise this question is trivial in that we can claim that there is a reflector buried in the medium as soon as the response matrix is not zero. In the presence of noise, it is not so obvious to answer this question since the response matrix is not zero due to additive noise even in the absence of a reflector. Our purpose is to build a detection test that has the maximal probability of detection for a given false alarm rate.
- where is the reflector ? This is the localization problem. Several methods can be proposed, essentially based on the back-propagation of the data set, and we will describe robust methods in the presence of noise.
- what are the characteristic properties of the reflector ? This is the reconstruction problem. One may look after geometric and physical properties. In fact, in view of the expression (1-2), only the product of the volume of the inclusion times the contrast can be identified in the regime we address in this paper.

The paper is organized as follows. In Section 3 we explain how the data should be collected to minimize the impact of the additive noise. In Section 4 we give results about the distribution of the singular values of the response matrix, with special attention on the maximal singular value. In Section 5 we discuss how the noise level can be estimated with minimal bias and variance. In Section 6 we build a test for the detection of the reflector and in Section 7 we show how the position and the scattering amplitude of the reflector can be estimated.

3 Data Acquisition

In this section we consider that there are M sources and N receivers. The measures are noisy, which means that the signal measured by a receiver is corrupted by an additive noise that can be described in terms of a circular complex Gaussian random variable with mean zero and variance $\sigma_{\rm n}^2$. The recorded noises are independent from each other.

In the standard acquisition scheme, the response matrix is measured during a sequence of M experiments. In the mth experience, $m = 1, \ldots, M$, the mth source (located at $\boldsymbol{z}_m$) generates a time-harmonic signal with unit amplitude and the N receivers (located at $\boldsymbol{y}_n$, $n = 1, \ldots, N$) record the backscattered waves which means that they measure

$$A_{{\rm meas},nm} = A_{0,nm} + W_{nm}, \quad n = 1, \ldots, N, \quad m = 1, \ldots, M,$$

which gives the matrix

$$\mathbf{A}_{\rm meas} = \mathbf{A}_0 + \mathbf{W}, \tag{9}$$

where $\mathbf{A}_0$ is the unperturbed response matrix of rank one (4) and W_{nm} are independent complex Gaussian random variables with mean zero and variance $\sigma_{\rm n}^2$.

The Hadamard technique is a noise reduction technique in the presence of additive noise that uses the structure of Hadamard matrices.

Definition 3.1 *A complex Hadamard matrix* $\mathbf{H}$ *of order* M *is a* $M \times M$ *matrix whose elements are of modulus one and such that* $\mathbf{H}^\dagger \mathbf{H} = M\mathbf{I}$.

Complex Hadamard matrices exist for all M. For instance the Fourier matrix

$$H_{nm} = \exp\Big[i2\pi \frac{(n-1)(m-1)}{M}\Big], \qquad m, n = 1, \ldots, M, \tag{10}$$

is a complex Hadamard matrix. A Hadamard matrix has maximal determinant among matrices with complex entries in the closed unit disk. More exactly Hadamard [21] proved that the determinant of any complex $M \times M$ matrix $\mathbf{H}$ with entries in the closed unit disk satisfies $|\det \mathbf{H}| \leq M^{M/2}$, with equality attained by a complex Hadamard matrix.

We now describe a general multi-source acquisition scheme and show the importance of Hadamard matrices to build an optimal scheme. Let $\mathbf{H}$ be an invertible $M \times M$ matrix with complex entries in the closed unit disk. In the multi-source acquisition scheme, the response matrix is measured during a sequence of M experiments. In the mth experience, $m = 1, \ldots, M$, all sources generate time-harmonic signals with unit amplitude (or smaller), the m' source generating $H_{m'm}$ for $m' = 1, \ldots, M$. In other words, in the mth experiment, we can use all the sources up to their maximal transmission power (that we have normalized to one) and we are free to choose their phases in order to minimize the effective noise level in the recorded data. In the mth experiment, the N receivers record the backscattered waves, which means that they measure

$$B_{\mathrm{meas},nm} = \sum_{m'=1}^{M} H_{m'm} A_{0,nm'} + W_{nm} = (\mathbf{A}_0 \mathbf{H})_{nm} + W_{nm}, \qquad n = 1, \ldots, N.$$

Collecting the recorded signals of the M experiments gives the matrix

$$\mathbf{B}_{\mathrm{meas}} = \mathbf{A}_0 \mathbf{H} + \mathbf{W},$$

where $\mathbf{A}_0$ is the unperturbed response matrix and W_{nm} are independent complex Gaussian random variables with mean zero and variance σ_{n}^2. The measured response matrix $\mathbf{A}_{\mathrm{meas}}$ is obtained by right multiplying the matrix $\mathbf{B}_{\mathrm{meas}}$ by the matrix $\mathbf{H}^{-1}$:

$$\mathbf{A}_{\mathrm{meas}} := \mathbf{B}_{\mathrm{meas}} \mathbf{H}^{-1} = \mathbf{A}_0 \mathbf{H} \mathbf{H}^{-1} + \mathbf{W} \mathbf{H}^{-1}, \tag{11}$$

so that we get the unperturbed matrix $\mathbf{A}_0$ up to a new noise

$$\mathbf{A}_{\mathrm{meas}} = \mathbf{A}_0 + \widetilde{\mathbf{W}}, \qquad \widetilde{\mathbf{W}} = \mathbf{W} \mathbf{H}^{-1}. \tag{12}$$

The choice of the matrix $\mathbf{H}$ should fulfill the property that the new noise matrix $\widetilde{\mathbf{W}}$ has independent complex entries with Gaussian statistics, mean zero, and minimal variance. We have

$$\begin{aligned} \mathbb{E}\Big[\overline{\widetilde{W}_{nm}} \widetilde{W}_{n'm'}\Big] &= \sum_{q,q'=1}^{M} \overline{(\mathbf{H}^{-1})_{qm}} (\mathbf{H}^{-1})_{q'm'} \mathbb{E}\big[\overline{W_{nq}} W_{n'q'}\big] \\ &= \sigma_{\mathrm{n}}^2 ((\mathbf{H}^{-1})^\dagger \mathbf{H}^{-1})_{mm'} \mathbf{1}_n(n'). \end{aligned}$$

This shows that we look for a complex matrix $\mathbf{H}$ with entries in the unit disk such that $(\mathbf{H}^{-1})^\dagger \mathbf{H}^{-1} = c\mathbf{I}$ with a minimal c. This is equivalent to require that $\mathbf{H}$ is unitary and that $|\det \mathbf{H}|$ is maximal. Using Hadamard result we know that the maximal determinant is $M^{M/2}$ and that a complex Hadamard matrix attains the maximum. Therefore a matrix $\mathbf{H}$ that minimizes the noise variance should be a Hadamard matrix, such as, for instance, the Fourier matrix (10). Note that, in the case of a linear array, the use of a Fourier matrix corresponds to an illumination in the form of plane waves with regularly sampled angles.

When the multi-source acquisition scheme is used with a Hadamard technique, we have $\mathbf{H}^{-1} = \frac{1}{M}\mathbf{H}^\dagger$ and the new noise matrix $\widetilde{\mathbf{W}}$ in (12) has independent complex entries with Gaussian statistics, mean zero, and variance $\sigma_{\rm n}^2/M$:

$$\mathbb{E}\Big[\overline{\widetilde{W}_{nm}}\widetilde{W}_{n'm'}\Big] = \frac{\sigma_{\rm n}^2}{M}\mathbf{1}_m(m')\mathbf{1}_n(n'). \tag{13}$$

This gain of a factor M in the signal-to-noise ratio is called the Hadamard advantage.

4 Singular Value Decomposition of the Response Matrix

4.1 Singular Values of a Noisy Matrix

We consider here the situation in which the measured response matrix $\mathbf{A}_{\rm meas}$ consists of independent noise coefficients with mean zero and variance $\sigma_{\rm n}^2/M$ and the number of receivers is larger than the number of sources $N \geq M$. As shown in the previous section, this is the case when the response matrix is acquired with the Hadamard technique and there is no reflector in the medium.

We denote by $\sigma_1^{(M)} \geq \sigma_2^{(M)} \geq \sigma_3^{(M)} \geq \cdots \geq \sigma_M^{(M)}$ the singular values of the response matrix $\mathbf{A}_{\rm meas}$ sorted by decreasing order and by $\Lambda^{(M)}$ the corresponding integrated density of states defined by

$$\Lambda^{(M)}([\sigma_u, \sigma_v]) := \frac{1}{M}\mathrm{Card}\left\{l = 1, \ldots, M\,,\, \sigma_l^{(M)} \in [\sigma_u, \sigma_v]\right\}, \qquad \text{for } \sigma_u < \sigma_v. \tag{14}$$

For large N and M with $N/M = \gamma \geq 1$ fixed we have the following results which are classical in random matrix theory [24, 23, 15].

Proposition 4.1 a) *The random measure $\Lambda^{(M)}$ almost surely converges to the deterministic absolutely continuous measure Λ with compact support:*

$$\Lambda([\sigma_u, \sigma_v]) = \int_{\sigma_u}^{\sigma_v} \frac{1}{\sigma_{\rm n}}\rho_\gamma\Big(\frac{\sigma}{\sigma_{\rm n}}\Big)d\sigma, \qquad 0 \leq \sigma_u \leq \sigma_v, \tag{15}$$

where ρ_γ is the deformed quarter-circle law given by

$$\rho_\gamma(x) = \begin{cases} \dfrac{1}{\pi x}\sqrt{\big((\gamma^{\frac12}+1)^2 - x^2\big)\big(x^2 - (\gamma^{\frac12}-1)^2\big)} & \text{if } \gamma^{\frac12} - 1 < x \leq \gamma^{\frac12} + 1, \\ 0 & \text{otherwise.} \end{cases} \tag{16}$$

b) *The normalized l^2-norm of the singular values satisfies*

$$M\Big[\frac{1}{M}\sum_{j=1}^{M}(\sigma_j^{(M)})^2 - \gamma\sigma_{\rm n}^2\Big] \overset{M\to\infty}{\longrightarrow} \sqrt{\gamma}\sigma_{\rm n}^2 Z_0 \text{ in distribution,} \tag{17}$$

where Z_0 follows a Gaussian distribution with mean zero and variance one.

c) *The maximal singular value satisfies*

$$M^{\frac23}\Big[\sigma_1^{(M)} - \sigma_{\rm n}\big(\gamma^{\frac12}+1\big)\Big] \overset{M\to\infty}{\longrightarrow} \frac{\sigma_{\rm n}}{2}\big(1+\gamma^{-\frac12}\big)^{\frac13} Z_2 \text{ in distribution,} \tag{18}$$

where Z_2 follows a type-2 Tracy Widom distribution.

The type-2 Tracy-Widom distribution has the cumulative distribution function Φ_{TW2} given by

$$\Phi_{\mathrm{TW2}}(z) = \exp\Big(- \int_z^\infty (x-z)\varphi^2(x)dx \Big), \tag{19}$$

where $\varphi(x)$ is the solution of the Painlevé equation

$$\varphi''(x) = x\varphi(x) + 2\varphi(x)^3, \quad \varphi(x) \simeq \mathrm{Ai}(x),\ x \to \infty, \tag{20}$$

Ai being the Airy function. The expectation of Z_2 is $\mathbb{E}[Z_2] \simeq -1.77$ and its variance is $\mathrm{Var}(Z_2) \simeq 0.81$. Detailed results about the Tracy-Widom distributions can be found in [11] and their numerical evaluations are addressed in [14].

4.2 Singular Values of the Perturbed Response Matrix

The measured response matrix using the Hadamard technique in the presence of a reflector and in the presence of measurement noise is

$$\mathbf{A}_{\mathrm{meas}} = \mathbf{A}_0 + \mathbf{W}, \tag{21}$$

where $\mathbf{A}_0$ is given by (4) and $\mathbf{W}$ has independent random complex entries with Gaussian statistics, mean zero and variance σ_{n}^2/M. We consider the critical and interesting regime in which the singular values of the unperturbed matrix are of the same order as the singular values of the noise, that is to say, σ_{ref} is of the same order of magnitude as σ_{n}. The following proposition shows that there is a phase transition:
- Either the noise level σ_{n} is smaller than the critical value $\gamma^{-1/4}\sigma_{\mathrm{ref}}$ and then the maximal singular value of the perturbed response matrix is a perturbation of the non-zero singular value of the unperturbed response matrix; this perturbation has Gaussian statistics with a mean of order one and a variance of the order of $1/M$.
- Or the noise level σ_{n} is larger than the critical value $\gamma^{-1/4}\sigma_{\mathrm{ref}}$ and then the non-zero singular value of the unperturbed response matrix is buried in the deformed quarter circle distribution of the pure noise matrix and the maximal singular value of the perturbed response matrix has a behavior similar to the pure noise case (described in Proposition 4.1).

Proposition 4.2 *In the regime $M \to \infty$:*

a) *The normalized l^2-norm of the singular values satisfies*

$$M\Big[\frac{1}{M}\sum_{j=1}^{M}(\sigma_j^{(M)})^2 - \gamma\sigma_{\mathrm{n}}^2\Big] \overset{M\to\infty}{\longrightarrow} \sigma_{\mathrm{ref}}^2 + \sqrt{2\gamma}\sigma_{\mathrm{n}}^2 Z_0 \text{ in distribution,} \tag{22}$$

where Z_0 follows a Gaussian distribution with mean zero and variance one.

b1) *If $\sigma_{\mathrm{ref}} < \gamma^{1/4}\sigma_{\mathrm{n}}$, then the maximal singular value satisfies*

$$\sigma_1^{(M)} \overset{M\to\infty}{\longrightarrow} \sigma_{\mathrm{n}}\big(\gamma^{\frac{1}{2}}+1\big) \text{ in probability.} \tag{23}$$

More exactly

$$M^{\frac{2}{3}}\Big[\sigma_1^{(M)} - \sigma_{\mathrm{n}}\big(\gamma^{\frac{1}{2}}+1\big)\Big] \overset{M\to\infty}{\longrightarrow} \frac{\sigma_{\mathrm{n}}}{2}\big(1+\gamma^{-\frac{1}{2}}\big)^{\frac{1}{3}} Z_2 \text{ in distribution,} \tag{24}$$

where Z_2 follows a type-2 Tracy Widom distribution.

b2) *If* $\sigma_{\mathrm{ref}} > \gamma^{1/4}\sigma_{\mathrm{n}}$, *then the maximal singular value satisfies*

$$\sigma_1^{(M)} \overset{M\to\infty}{\longrightarrow} \sigma_{\mathrm{ref}}\big(1+\gamma\frac{\sigma_{\mathrm{n}}^2}{\sigma_{\mathrm{ref}}^2}\big)^{\frac{1}{2}}\big(1+\frac{\sigma_{\mathrm{n}}^2}{\sigma_{\mathrm{ref}}^2}\big)^{\frac{1}{2}} \text{ in probability.} \tag{25}$$

More exactly

$$M^{\frac{1}{2}}\Big[\sigma_1^{(M)} - \sigma_{\mathrm{ref}}\big(1+\gamma\frac{\sigma_{\mathrm{n}}^2}{\sigma_{\mathrm{ref}}^2}\big)^{\frac{1}{2}}\big(1+\frac{\sigma_{\mathrm{n}}^2}{\sigma_{\mathrm{ref}}^2}\big)^{\frac{1}{2}}\Big] \overset{M\to\infty}{\longrightarrow} \frac{\sigma_{\mathrm{n}}}{2}\frac{\big(1-\gamma\frac{\sigma_{\mathrm{n}}^4}{\sigma_{\mathrm{ref}}^4}\big)^{\frac{1}{2}}\big(2+(1+\gamma)\frac{\sigma_{\mathrm{n}}^2}{\sigma_{\mathrm{ref}}^2}\big)^{\frac{1}{2}}}{\big(1+\gamma\frac{\sigma_{\mathrm{n}}^2}{\sigma_{\mathrm{ref}}^2}\big)^{\frac{1}{2}}\big(1+\frac{\sigma_{\mathrm{n}}^2}{\sigma_{\mathrm{ref}}^2}\big)^{\frac{1}{2}}}Z_0, \tag{26}$$

in distribution, where Z_0 *follows a Gaussian distribution with mean zero and variance one.*

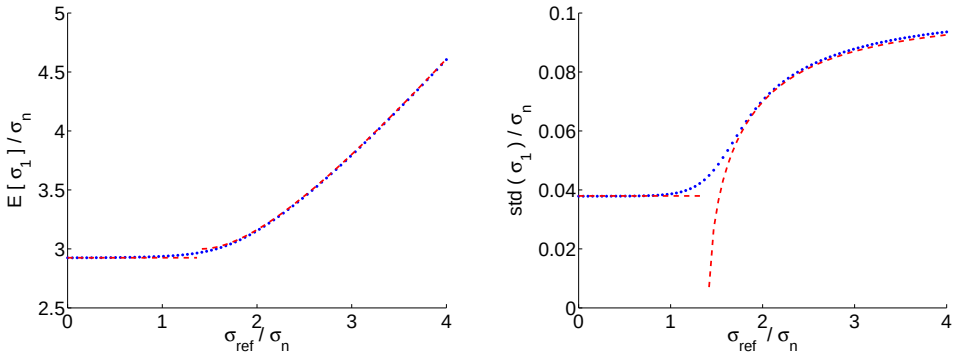

Figure 1: Mean and standard deviation of the maximal singular value. We compare the empirical means (left) and standard deviations (right) obtained from 10^4 MC simulations (blue dots) with the theoretical formulas given in Proposition 4.2 (red dashed lines). Here $N = 200$ and $M = 50$ ($\gamma = 4$).

These results are illustrated in Figure 1. Their proofs can be obtained from the method described in [13]. Note however that, although the method used in [13] is correct, Theorem 2.19 there gives a formula for the asymptotic variance that seems in disagreement with our formula (26). Our numerical simulations indicate however that our formula seems correct (and is quite far from the formula in [13]). Extensions to heteroscedastic noise can also be obtained as in [16]. Note that formula (26) seems to predict that the standard deviation of the maximal singular value cancels when $\sigma_{\mathrm{ref}} \searrow \gamma^{1/4}\sigma_{\mathrm{n}}$, but this is true only to the order $M^{-1/2}$, and in fact it becomes of order $M^{-2/3}$ (see Figure 1). Following [10] we can anticipate that there are interpolating distributions which appear when $\sigma_{\mathrm{ref}} = \gamma^{1/4}\sigma_{\mathrm{n}} + wM^{-1/3}$ for some fixed w. This problem deserves a detailed study.

4.3 Singular Vectors of the Perturbed Response Matrix

It is of interest to describe the statistical distribution of the angle between the left singular vector $\boldsymbol{u}_1^{(M)}$ (resp. right singular vector $\boldsymbol{v}_1^{(M)}$) of the noisy matrix $\mathbf{A}_{\mathrm{meas}}$ and the left singular vector $\boldsymbol{u}(\boldsymbol{x}_{\mathrm{ref}})$ (resp. right singular vector $\boldsymbol{v}(\boldsymbol{x}_{\mathrm{ref}})$) of the unperturbed matrix $\mathbf{A}_0$. This justifies the MUSIC-based algorithm for the reflector localization algorithm that we discuss in Section 7.1.

Proposition 4.3 *We consider the case* $\sigma_{\mathrm{ref}} > \gamma^{\frac{1}{4}}\sigma_{\mathrm{n}}$. *When* $\gamma = N/M$ *is fixed and* $M \to \infty$, *we have in probability*

$$\big|(\boldsymbol{u}_1^{(M)})^\dagger \boldsymbol{u}(\boldsymbol{x}_{\mathrm{ref}})\big|^2 \overset{M\to\infty}{\longrightarrow} \frac{1-\gamma\frac{\sigma_{\mathrm{n}}^4}{\sigma_{\mathrm{ref}}^4}}{1+\gamma\frac{\sigma_{\mathrm{n}}^2}{\sigma_{\mathrm{ref}}^2}} \quad \text{and} \quad \big|(\boldsymbol{v}_1^{(M)})^\dagger \boldsymbol{v}(\boldsymbol{x}_{\mathrm{ref}})\big|^2 \overset{M\to\infty}{\longrightarrow} \frac{1-\gamma\frac{\sigma_{\mathrm{n}}^4}{\sigma_{\mathrm{ref}}^4}}{1+\frac{\sigma_{\mathrm{n}}^2}{\sigma_{\mathrm{ref}}^2}}. \tag{27}$$

Proposition 4.3 shows that the first singular vectors of the perturbed matrix $\mathbf{A}_{\text{meas}}$ have deterministic angles with respect to the first singular vectors of the unperturbed matrix $\mathbf{A}_0$ provided the first singular value emerges from the deformed quarter-circle distribution. These results are proved in [13] and they are illustrated in Figure 2.

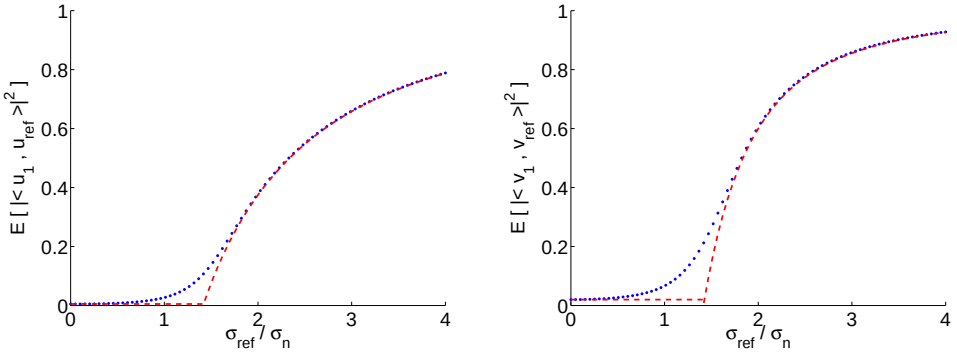

Figure 2: Means of the square angles between the perturbed and unperturbed singular vectors. We compare the empirical means obtained from 10^4 MC simulations (blue dots) with the theoretical formulas given in Proposition 4.3 (red dashed lines). Here $N = 200$ and $M = 50$ ($\gamma = 4$).

5 The Evaluation of the Noise Level

5.1 Empirical Estimator

The truncated normalized l^2-norm of the singular values satisfies (22). Therefore the truncated normalized l^2-norm of the singular values satisfies

$$M\Big[\frac{1}{M-(1+\gamma^{-\frac{1}{2}})^2}\sum_{j=2}^{M}(\sigma_j^{(M)})^2-\gamma\sigma_{\text{n}}^2\Big]\overset{M\to\infty}{\longrightarrow} b_1+\sqrt{\gamma}\sigma_{\text{n}}^2 Z_0 \text{ in distribution,}$$

where Z_0 follows a Gaussian distribution with mean zero and variance one, and the asymptotic bias is

$$b_1=\sigma_{\text{ref}}^2-\bar{\sigma}_1^2+\sigma_{\text{n}}^2(1+\gamma^{\frac{1}{2}})^2. \tag{28}$$

Here

$$\bar{\sigma}_1=\max\Big\{\sigma_{\text{ref}}\big(1+\gamma\frac{\sigma_{\text{n}}^2}{\sigma_{\text{ref}}^2}\big)^{\frac{1}{2}}\big(1+\frac{\sigma_{\text{n}}^2}{\sigma_{\text{ref}}^2}\big)^{\frac{1}{2}},\ \sigma_{\text{n}}(1+\gamma^{\frac{1}{2}})\Big\} \tag{29}$$

is the deterministic leading-order value of the maximal singular value as shown in Proposition 4.2. The normalization in the truncated l^2-norm has been chosen so that, in the absence of a reflector, the asymptotic bias is zero: $b_1\,|_{\sigma_{\text{ref}}=0}=0$. This implies that

$$\hat{\sigma}_{\text{n}}^e:=\gamma^{-\frac{1}{2}}\Big[\frac{1}{M-(1+\gamma^{-\frac{1}{2}})^2}\sum_{j=2}^{M}(\sigma_j^{(M)})^2\Big]^{\frac{1}{2}} \tag{30}$$

is an empirical estimator of σ_{n} with Gaussian fluctuations of the order of M^{-1}. This estimator satisfies

$$M\Big[\hat{\sigma}_{\text{n}}^e-\sigma_{\text{n}}\Big]\overset{M\to\infty}{\longrightarrow}\frac{b_1}{2\gamma\sigma_{\text{n}}}+\frac{\sigma_{\text{n}}}{2\gamma^{\frac{1}{2}}}Z_0 \text{ in distribution,}$$

and therefore

$$\hat{\sigma}_{\mathrm{n}}^{e} = \sigma_{\mathrm{n}} + o(\frac{1}{M^{\frac{2}{3}}}) \text{ in probability.} \tag{31}$$

The empirical estimator is easy to compute, since it requires the evaluation of the Frobenius norm of the measured matrix $\mathbf{A}_{\mathrm{meas}}$ and the maximal singular value:

$$\hat{\sigma}_{\mathrm{n}}^{e} = \gamma^{-\frac{1}{2}} \Big[\frac{\sum_{n=1}^{N} \sum_{m=1}^{M} |A_{nm}|^2 - (\sigma_1^{(M)})^2}{M - (1+\gamma^{-\frac{1}{2}})^2} \Big]^{\frac{1}{2}}. \tag{32}$$

5.2 Corrected Empirical Estimator

It is possible to improve the quality of the estimation of the noise level and to cancel the bias of the empirical estimator. Using Proposition 4.2 we can see that the quantity

$$\hat{\sigma}_{\mathrm{ref}}^{e} = \frac{\hat{\sigma}_{\mathrm{n}}^{e}}{\sqrt{2}} \Big\{ \Big(\frac{\sigma_1^{(M)}}{\hat{\sigma}_{\mathrm{n}}^{e}} \Big)^2 - 1 - \gamma + \Big(\Big[\Big(\frac{\sigma_1^{(M)}}{\hat{\sigma}_{\mathrm{n}}^{e}} \Big)^2 - 1 - \gamma \Big]^2 - 4\gamma \Big)^{\frac{1}{2}} \Big\}^{\frac{1}{2}} \tag{33}$$

is an estimator of σ_{ref}, provided that $\sigma_{\mathrm{ref}} > \gamma^{1/4}\sigma_{\mathrm{n}}$. Therefore, when $\sigma_{\mathrm{ref}} > \gamma^{1/4}\sigma_{\mathrm{n}}$, it is possible to build an improved estimator of the noise variance by removing from the empirical estimator an estimation of the asymptotic bias which is itself based on the empirical estimator $\hat{\sigma}_{\mathrm{n}}^{e}$. The estimator of the asymptotic bias that we propose to use is

$$\hat{b}_1^{e} = (\hat{\sigma}_{\mathrm{ref}}^{e})^2 - (\sigma_1^{(M)})^2 + (\hat{\sigma}_{\mathrm{n}}^{e})^2 (1+\gamma^{\frac{1}{2}})^2, \tag{34}$$

and therefore we can propose the following estimator of the noise level σ_{n}:

$$\hat{\sigma}_{\mathrm{n}}^{c} := \hat{\sigma}_{\mathrm{n}}^{e} - \frac{\hat{b}_1^{e}}{2\gamma M \hat{\sigma}_{\mathrm{n}}^{e}}. \tag{35}$$

This estimator satisfies

$$M \Big[\hat{\sigma}_{\mathrm{n}}^{c} - \sigma_{\mathrm{n}} \Big] \overset{M\to\infty}{\longrightarrow} \frac{\sigma_{\mathrm{n}}}{2\gamma^{\frac{1}{2}}} Z_0 \text{ in distribution.} \tag{36}$$

This estimator can only be used when $\hat{\sigma}_{\mathrm{ref}}^{e} > \gamma^{1/4}\hat{\sigma}_{\mathrm{n}}^{e}$ and it should then be preferred to the empirical estimator $\hat{\sigma}_{\mathrm{n}}^{e}$.

5.3 Kolmogorov-Smirnov Estimator

An alternative method to estimate σ_{n} is the approach outlined in [20] and applied in [25], which consists in minimizing the Kolmogorov-Smirnov distance $\mathcal{D}(\sigma)$ between the observed sample distribution of the $M-K$ smallest singular values of the measured matrix $\mathbf{A}_{\mathrm{meas}}$ and that predicted by theory, which is the deformed quarter circle distribution (16) parameterized by σ_{n}. Compared to [20, 25] we here introduce a cut-off parameter K that can be chosen by the user. All choices are equivalent in the asymptotic framework $M \to \infty$, but for finite M low values for K give estimators with small variances but with bias, while large values for K increase the variance but decay the bias (see Figure 3). We define the new estimator $\hat{\sigma}_{\mathrm{n}}^{K}$ of σ_{n} as the parameter that minimizes the Kolmogorov-Smirnov distance. After elementary manipulations we find that the Kolmogorov-Smirnov estimator is of the form

$$\hat{\sigma}_{\mathrm{n}}^{K} := \operatorname*{argmin}_{\sigma>0} \mathcal{D}_K^{(M)}(\sigma), \tag{37}$$

where $\mathcal{D}_K^{(M)}(\sigma)$ is defined by:

$$\mathcal{D}_K^{(M)}(\sigma) := \max_{m=1,\dots,M-K} \Big| G_\gamma \Big(\frac{\sigma_{M+1-m}^{(M)}}{\sigma} \Big) - \frac{m-1/2}{M} \Big| + \frac{1}{2M}, \tag{38}$$

G_γ is the cumulative distribution function with density (16):

$$G_\gamma(x) = \begin{cases} 0 & \text{if } x \leq \gamma^{\frac{1}{2}} - 1, \\ \frac{1}{2} + \frac{\gamma^{\frac{1}{2}}}{\pi}\big(1 - G(x)^2\big)^{\frac{1}{2}} - \frac{\gamma+1}{\pi}\arcsin\big(G(x)\big) & \\ \quad -\frac{\gamma-1}{\pi}\arctan\Big(\frac{1-(\gamma^{\frac{1}{2}}+\gamma^{-\frac{1}{2}})G(x)}{(1-G(x)^2)^{\frac{1}{2}}(\gamma^{\frac{1}{2}}-\gamma^{-\frac{1}{2}})}\Big) & \text{if } \gamma^{\frac{1}{2}} - 1 < x \leq \gamma^{\frac{1}{2}} + 1, \\ 1 & \text{if } \gamma^{\frac{1}{2}} + 1 < x, \end{cases}$$

with

$$G(x) = \frac{(1+\gamma) - x^2}{2\gamma^{\frac{1}{2}}}.$$

If $\gamma = 1$, then we have

$$G_1(x) = \begin{cases} 0 & \text{if } x \leq 0, \\ \frac{1}{2\pi}\Big(x\sqrt{4-x^2} + 4\arcsin\big(\frac{x}{2}\big)\Big) & \text{if } 0 < x \leq 2, \\ 1 & \text{if } 2 < x. \end{cases}$$

5.4 Discussion

The three estimation methods described in the three previous subsections have been implemented and numerical results are reported in Figure 3.

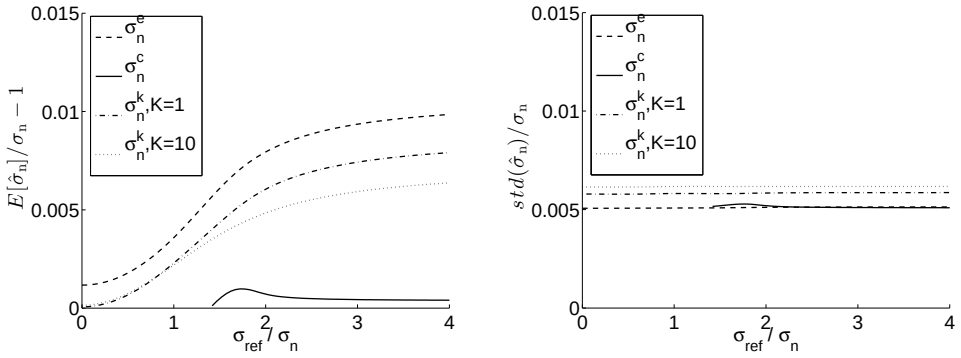

Figure 3: Relative bias (left) and standard deviations (right) of different estimators of the noise level. Here $N = 200$ and $M = 50$ ($\gamma = 4$).

As predicted by the asymptotic theory, the variance of the empirical estimator is equivalent to the one of the corrected empirical estimator, and they are smaller than the ones of the Kolmogorov-Smirnov estimator. The bias of the empirical estimator is larger than the bias of the Kolmogorov-Smirnov estimator. The corrected empirical estilmator has a very small bias. The variance of the Kolmogorov-Smirnov estimator increases with K, but its bias decreases with increasing K. From these observations it turns out that:
- when $\hat{\sigma}^e_{\text{ref}} > \gamma^{1/4}\hat{\sigma}^e_{\text{n}}$, then it is recommended to use the corrected empirical estimator (35). It is the one that has the minimal bias and the minimal variance amongst all the estimators studied in this paper, but it can only be applied in the regime when the singular value corresponding to the reflector is outside the deformed quarter-circle distribution of the noise singular values.
- when $\hat{\sigma}^e_{\text{ref}} < \gamma^{1/4}\hat{\sigma}^e_{\text{n}}$, then it is recommended to use the Kolmogorov-Smirnov estimator (37) with $K = 1$. Although its variance is larger than the one of the empirical estimator, its bias is much smaller and, as a result, it is the one that has the minimal quadratic error (sum of the squared bias and of the variance).

To summarize, the estimator of the noise variance that we will use in the following is:

$$\hat{\sigma}_{\mathrm{n}}^{f} = \mathbf{1}_{\hat{\sigma}_{\mathrm{ref}}^{e} \leq \gamma^{1/4}\hat{\sigma}_{\mathrm{n}}^{e}} \hat{\sigma}_{\mathrm{n}}^{K=1} + \mathbf{1}_{\hat{\sigma}_{\mathrm{ref}}^{e} > \gamma^{1/4}\hat{\sigma}_{\mathrm{n}}^{e}} \hat{\sigma}_{\mathrm{n}}^{c}. \tag{39}$$

Its bias and standard deviation are plotted in Figure 4.

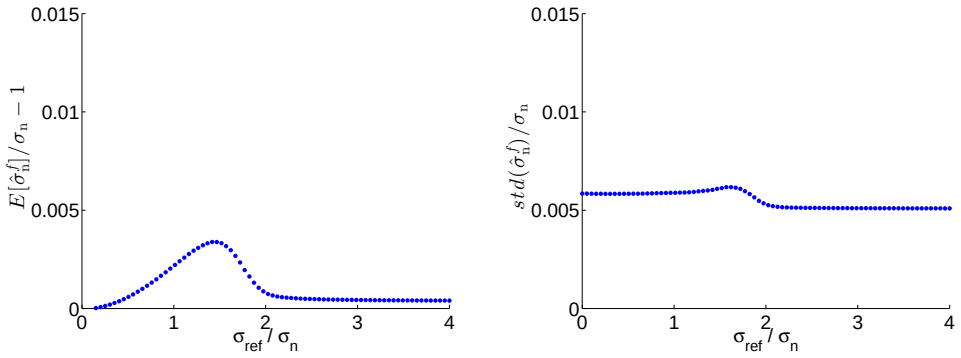

Figure 4: Relative bias (left) and standard deviations (right) of the final estimator (39) of the noise level. Here $N = 200$ and $M = 50$ ($\gamma = 4$).

6 Detection Test

Consider the response matrix in the presence of measurement noise:

$$\mathbf{A}_{\mathrm{meas}} = \mathbf{A}_0 + \mathbf{W},$$

where $\mathbf{A}_0$ is zero in the absence of a reflector and equal to (4) when there is a reflector. The matrix $\mathbf{W}$ models additive measurement noise and its complex entries are independent and identically distributed with Gaussian statistics, mean zero and variance σ_{n}^2/M.

The objective is to propose a detection test for the reflector. Since we know that the presence of a reflector is characterized by the existence of a significant singular value, we propose to use a test of the form $R > r$ for the alarm corresponding to the presence of a reflector. Here R is the quantity obtained from the measured response matrix and defined by

$$R = \frac{\sigma_1^{(M)}}{\hat{\sigma}_{\mathrm{n}}}, \tag{40}$$

where $\hat{\sigma}_{\mathrm{n}}$ is the known value of σ_{n}, if known, or the estimator (39) of σ_{n}. Here the threshold value r of the test has to be chosen by the user. This choice follows from Neyman-Pearson theory as we explain below. It requires the knowledge of the statistical distribution of R which we give in the following proposition, which is a corollary of Proposition 4.2 (and Slutsky's theorem).

Proposition 6.1 *In the asymptotic regime $M \gg 1$ the following statements hold.*

a) *In absence of a reflector we have up to a term of order $o(M^{-2/3})$:*

$$R \simeq 1 + \gamma^{\frac{1}{2}} + \frac{1}{2M^{\frac{2}{3}}}\left(1 + \gamma^{-\frac{1}{2}}\right)^{\frac{1}{3}} Z_2, \tag{41}$$

where Z_2 follows a type-2 Tracy Widom distribution.

b) *In presence of a reflector:*

b1) *If* $\sigma_{\rm ref} > \gamma^{1/4}\sigma_{\rm n}$*, then we have up to a term of order* $o(M^{-1/2})$*:*

$$R \simeq \frac{\sigma_{\rm ref}}{\sigma_{\rm n}}\big(1+\gamma\frac{\sigma_{\rm n}^2}{\sigma_{\rm ref}^2}\big)^{\frac{1}{2}}\big(1+\frac{\sigma_{\rm n}^2}{\sigma_{\rm ref}^2}\big)^{\frac{1}{2}} + \frac{1}{2M^{\frac{1}{2}}}\Big(\frac{\big(1-\gamma\frac{\sigma_{\rm n}^4}{\sigma_{\rm ref}^4}\big)\big(2+(1+\gamma)\frac{\sigma_{\rm n}^2}{\sigma_{\rm ref}^2}\big)}{\big(1+\gamma\frac{\sigma_{\rm n}^2}{\sigma_{\rm ref}^2}\big)\big(1+\frac{\sigma_{\rm n}^2}{\sigma_{\rm ref}^2}\big)^{\frac{1}{2}}}\Big)^{\frac{1}{2}} Z_0, \quad (42)$$

where Z_0 *follows a Gaussian distribution with mean zero and variance one.*

b2) *If* $\sigma_{\rm ref} < \gamma^{1/4}\sigma_{\rm n}$*, then we have (41).*

The data (i.e. the measured response matrix) gives the value of the ratio R. We propose to use a test of the form $R > r$ for the alarm corresponding to the presence of a reflector. The quality of this test can be quantified by two coefficients:
- The false alarm rate (FAR) is the probabilty to sound the alarm while there is no reflector:

$$\text{FAR} = \mathbb{P}(R > r_\alpha | \text{ no reflector }).$$

- The probability of detection (POD) is the probability to sound the alarm when there is a reflector:

$$\text{POD} = \mathbb{P}(R > r_\alpha | \text{ reflector }).$$

As is well-known in statistical test theory, it is not possible to find a test that minimizes the FAR and maximizes the POD. However, by the Neyman-Pearson lemma, the decision rule of sounding the alarm if and only if $R > r_\alpha$ maximizes the POD for a given FAR α, provided the threshold is taken to be equal to

$$r_\alpha = 1 + \gamma^{\frac{1}{2}} + \frac{1}{2M^{\frac{2}{3}}}\big(1+\gamma^{-\frac{1}{2}}\big)^{\frac{1}{3}}\Phi_{\rm TW2}^{-1}(1-\alpha), \quad (43)$$

where $\Phi_{\rm TW2}$ is the cumulative distribution function (19) of the Tracy-Widom distribution of type 2. The computation of the threshold r_α is easy since it depends only on the number of sensors N and M and on the FAR α. We have, for instance, $\Phi_{\rm TW2}^{-1}(0.9) \simeq -0.60$, $\Phi_{\rm TW2}^{-1}(0.95) \simeq -0.23$ and $\Phi_{\rm TW2}^{-1}(0.99) \simeq 0.48$. These values are used in the detection tests whose POD are plotted in Figure 5.

The POD of this optimal test (optimal amongst all tests with the FAR α) depends on the value $\sigma_{\rm ref}$ and on the noise level $\sigma_{\rm n}$. The theoretical test performance improves very rapidly with M when $\sigma_{\rm ref} > \gamma^{1/4}\sigma_{\rm n}$. When $\sigma_{\rm ref} < \gamma^{1/4}\sigma_{\rm n}$, so that the reflector is buried in noise (more exactly, the singular value corresponding to the reflector is buried in the deformed quarter-circle distribution of the other singular values), then we have $\text{POD} = 1 - \Phi_{\rm TW2}\big(\Phi_{\rm TW2}^{-1}(1-\alpha)\big) = \alpha$.

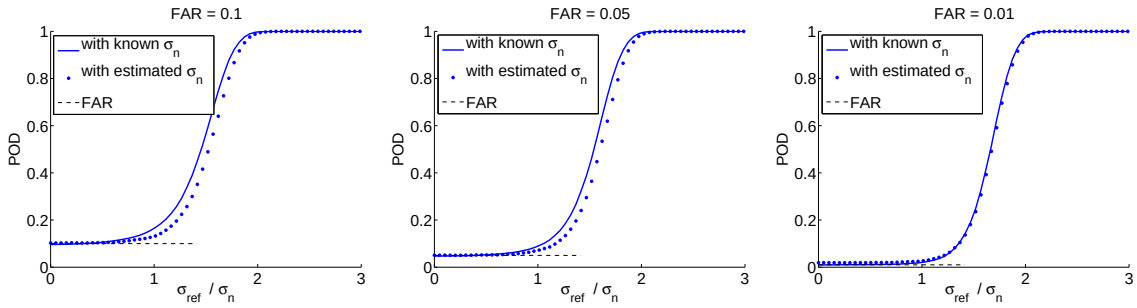

Figure 5: Probability of detection (POD) for the detection test calibrated with the threshold values r_α with $\alpha = 0.1$ (left), $\alpha = 0.05$ (center), and $\alpha = 0.01$ (right). Here $N = 200$ and $M = 50$. The blue solid and dotted lines correspond to the results of 10^4 MC simulations, in which the noise level is known (thick solid lines) or estimated by (39) (thick dotted lines). The dashed lines are the FAR desired in the absence of a reflector, that should be obtained when $\sigma_{\rm ref} = 0$.

The POD of the test (40) calibrated for different values of the FAR is plotted in Figure 5. One can observe that the calibration with r_α gives the desired FAR and that the POD rapidly goes to one when the singular value σ_{ref} of the reflector becomes larger than $\gamma^{1/4}\sigma_{\text{n}}$. Furthermore, the use of the estimator (39) for the noise level σ_{n} is also very efficient in that we get almost the same FAR and POD with the true value σ_{n} as with the estimator $\hat{\sigma}_{\text{n}}^f$. In Figure 6 we plot the POD obtained with other estimators of the noise level in order to confirm that the estimator $\hat{\sigma}_{\text{n}}^f$ defined by (39) is indeed the most appropriate.

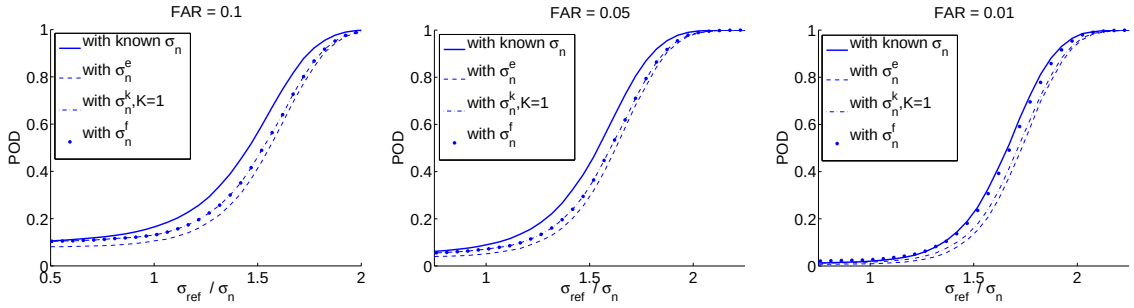

Figure 6: Probability of detection (POD) for the detection test calibrated with the threshold values r_α with $\alpha = 0.1$ (left), $\alpha = 0.05$ (center), and $\alpha = 0.01$ (right). Here $N = 200$ and $M = 50$. The blue lines correspond to the results of 10^4 MC simulations, in which the noise level is known (thick solid lines) or estimated by (39) (thick dotted lines) or estimated by the estimators (30) and (37) (thin dashed lines).

7 Target Localization and Reconstruction

In this section we would like to present simple and robust way to localize the reflector and reconstruct its properties once the detection test has passed. By simple we mean that we will only use the first singular value and left singular vector of the response matrix, and by robust we mean a procedure that allows for estimations with bias and variance as small as possible.

7.1 Localization

A standard imaging functional is the MUSIC functional defined by [1]

$$\mathcal{I}_{\text{MUSIC}}(\boldsymbol{x}) \quad := \quad \left\| \boldsymbol{u}(\boldsymbol{x}) - \left({\boldsymbol{u}_1^{(M)}}^\dagger \boldsymbol{u}(\boldsymbol{x}) \right) \boldsymbol{u}_1^{(M)} \right\|^{-\frac{1}{2}} = \left(1 - \left| \boldsymbol{u}(\boldsymbol{x})^\dagger \boldsymbol{u}_1^{(M)} \right|^2 \right)^{-\frac{1}{2}},$$

where $\boldsymbol{u}(\boldsymbol{x})$ is the normalized vector of Green's functions (8) and $\boldsymbol{u}_1^{(M)}$ is the first left singular vector of the measured response matrix $\mathbf{A}_{\text{meas}}$. The MUSIC functional is the projection of the Green's vector $\boldsymbol{u}(\boldsymbol{x})$ from the receiver array to the search point $\boldsymbol{x}$ onto the noise space of the measured response matrix.

In the absence of noise the MUSIC functional presents a peak at $\boldsymbol{x} = \boldsymbol{x}_{\text{ref}}$. Indeed, in this case, we have $\boldsymbol{u}_1^{(M)} = \boldsymbol{u}(\boldsymbol{x}_{\text{ref}})$ (up to a phase term) and therefore $\mathcal{I}_{\text{MUSIC}}(\boldsymbol{x})$ becomes singular at $\boldsymbol{x} = \boldsymbol{x}_{\text{ref}}$. Furthermore, we can quantify the accuracy of the reflector localization as follows. When the arrays surround the search region, the singular vectors $\boldsymbol{u}(\boldsymbol{x})$ can be shown to be orthogonal to $\boldsymbol{u}(\boldsymbol{x}_{\text{ref}})$ when the distance between the search point $\boldsymbol{x}$ and the reflector point $\boldsymbol{x}_{\text{ref}}$ becomes larger than half-a-wavelength. This can be shown using Hemlholtz-Kirchhoff identity and this gives the resolution of the imaging functional: one can get the position of the reflector within the accuracy of half-a-wavelength. When the arrays are partial, then the accuracy can be described in terms of the so-called Rayleigh resolution formulas [17, 19].

In the presence of noise the peak of the MUSIC functional is affected. By Proposition 4.3, in the regime $M \gg 1$, the value of the MUSIC functional at an arbitrary point $\boldsymbol{x} \neq \boldsymbol{x}_{\rm ref}$ is one while the theoretical value at $\boldsymbol{x} = \boldsymbol{x}_{\rm ref}$ is given by

$$\mathcal{I}_{\rm MUSIC}(\boldsymbol{x}_{\rm ref}) = (1 - c_u)^{-\frac{1}{2}},$$

where c_u is the theoretical angle between the first left singular vector $\boldsymbol{u}(\boldsymbol{x}_{\rm ref})$ of the unperturbed matrix $\mathbf{A}_0$ and the first left singular vector $\boldsymbol{u}_1^{(M)}$ of the measured response matrix $\mathbf{A}_{\rm meas}$:

$$c_u = \begin{cases} \dfrac{1 - \gamma \frac{\sigma_{\rm n}^4}{\sigma_{\rm ref}^4}}{1 + \gamma \frac{\sigma_{\rm n}^2}{\sigma_{\rm ref}^2}} & \text{if } \sigma_{\rm ref} > \gamma^{\frac{1}{4}} \sigma_{\rm n}, \\ 0 & \text{if } \sigma_{\rm ref} < \gamma^{\frac{1}{4}} \sigma_{\rm n}. \end{cases}$$

Therefore, provided the detection test has passed, which means that the reflector singular value is larger than the noise singular values, the MUSIC algorithm gives a robust and simple way to estimate the position of the reflector. The estimator of $\boldsymbol{x}_{\rm ref}$ that we propose is

$$\hat{\boldsymbol{x}}_{\rm ref} := \operatorname*{argmax}_{\boldsymbol{x}} \mathcal{I}_{\rm MUSIC}(\boldsymbol{x}). \tag{44}$$

Note that more complex and computationally expensive algorithms (using reverse-time migration) can improve the quality of the estimation as shown in [2].

7.2 Reconstruction

Using Proposition 4.2 we can see that the quantity

$$\hat{\sigma}_{\rm ref} = \frac{\hat{\sigma}_{\rm n}}{\sqrt{2}} \Big\{ \Big(\frac{\sigma_1^{(M)}}{\hat{\sigma}_{\rm n}} \Big)^2 - 1 - \gamma + \Big(\Big[\Big(\frac{\sigma_1^{(M)}}{\hat{\sigma}_{\rm n}} \Big)^2 - 1 - \gamma \Big]^2 - 4\gamma \Big)^{\frac{1}{2}} \Big\}^{\frac{1}{2}} \tag{45}$$

is an estimator of $\sigma_{\rm ref}$, provided that $\sigma_{\rm ref} > \gamma^{\frac{1}{4}} \sigma_{\rm n}$. Here $\hat{\sigma}_{\rm n}$ is the known value of $\sigma_{\rm n}$, if known, or the estimator (39) of $\sigma_{\rm n}$. In practice, if the detection test passes, then this implies that we are in this case. From (6) we can therefore estimate the scattering amplitude $\rho_{\rm ref}$ of the inclusion by

$$\hat{\rho}_{\rm ref} = \frac{c_0^2}{\omega^2} \Big(\sum_{n=1}^{N} |\hat{G}(\omega, \hat{\boldsymbol{x}}_{\rm ref}, \boldsymbol{y}_n)|^2 \Big)^{-\frac{1}{2}} \Big(\sum_{m=1}^{M} |\hat{G}(\omega, \hat{\boldsymbol{x}}_{\rm ref}, \boldsymbol{z}_m)|^2 \Big)^{-\frac{1}{2}} \hat{\sigma}_{\rm ref}, \tag{46}$$

with $\hat{\sigma}_{\rm ref}$ the estimator (45) of $\sigma_{\rm ref}$ and $\hat{\boldsymbol{x}}_{\rm ref}$ is the estimator (44) of the position of the inclusion. This estimator is not biased asymptotically because it compensates for the level repulsion of the first singular value due to the noise.

7.3 Numerical Simulations

We consider the following numerical set-up: the wavelength is equal to one. There is one reflector with scattering amplitude $\rho_{\rm ref} = 1$, located at $\boldsymbol{x}_{\rm ref} = (0, 0, 50)$. We consider a linear array of $N = 200$ transducers located at half-a-wavelength apart on the line from $(-50, 0, 0)$ to $(50, 0, 0)$. Each transducer is used as a receiver, but only one of four is used as a source (therefore, $M = 50$ and $\gamma = 4$). The noise level is $\sigma_{\rm n} = \sigma_{\rm ref}/4$ or $\sigma_{\rm ref}/2$, where $\sigma_{\rm ref}$ is the singular value associated to the reflector (given by (6)).

We have carried out a series of 10^4 MC simulations (using the estimator (39) of $\sigma_{\rm n}$). The results are reported in Figure 7 (for $\sigma_{\rm n} = \sigma_{\rm ref}/4$) and in Figure 8 (for $\sigma_{\rm n} = \sigma_{\rm ref}/2$):

- the reflector is always detected when $\sigma_{\rm n} = \sigma_{\rm ref}/4$ and it is detected with probability 97% when $\sigma_{\rm n} = \sigma_{\rm ref}/2$ (in agreement with the POD plotted in Figure 5).

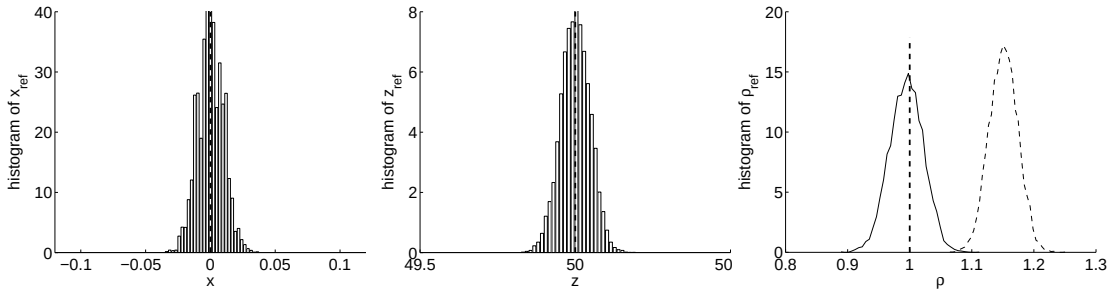

Figure 7: Left: Histogram of the estimated cross-range position $\hat{x}_{\rm ref}$ given by (44). Center: Histogram of the estimated range position $\hat{z}_{\rm ref}$ given by (44). Right: Histogram of the estimated scattering amplitude $\hat{\rho}_{\rm ref}$ given by (46) (solid lines) or $\hat{\rho}^e_{\rm ref}$ given by (47) (dashed lines). Here $\sigma_{\rm n} = \sigma_{\rm ref}/4$.

- the estimator $\hat{\boldsymbol{x}}_{\rm ref}$ defined by (44) of the position of the reflector has good properties. The histograms of the estimated positions $\hat{\boldsymbol{x}}_{\rm ref} = (\hat{x}_{\rm ref}, 0, \hat{z}_{\rm ref})$ are plotted in Figures 7-8 (left and center).

- the estimator $\hat{\rho}_{\rm ref}$ defined by (46) of the scattering amplitude has no bias because it uses the inversion formula (45) which compensates for the level repulsion of the first singular value. We plot in Figures 7-8 (right) the histogram of the estimated scattering amplitude and we compare with the empirical estimator

$$\hat{\rho}^e_{\rm ref} = \frac{c_0^2}{\omega^2}\Big(\sum_{n=1}^{N} |\hat{G}(\omega, \hat{\boldsymbol{x}}_{\rm ref}, \boldsymbol{y}_n)|^2\Big)^{-\frac{1}{2}}\Big(\sum_{m=1}^{M} |\hat{G}(\omega, \hat{\boldsymbol{x}}_{\rm ref}, \boldsymbol{z}_m)|^2\Big)^{-\frac{1}{2}}\sigma_1^{(M)}, \tag{47}$$

which has a large bias.

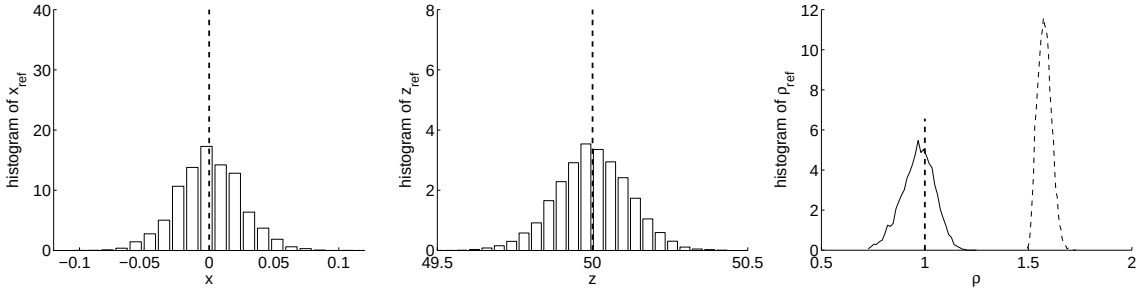

Figure 8: The same as in Figure 7, but here $\sigma_{\rm n} = \sigma_{\rm ref}/2$.

8 Conclusion

In this paper we have presented a few results that show how random matrix theory can be used in sensor array imaging. It turns out that most of the needed results are already available in the literature in the case addressed in this paper, i.e. when the response matrix is perturbed by an additive measurement noise. However, the most interesting questions arise in the presence of clutter noise, which is the case in which the data are corrupted by perturbations due to random heterogeneities present in the medium. In this case the random perturbation of the response matrix cannot be described in terms of an additive uncorrelated noise, but it has special correlation structure [9, 18]. This case certainly deserves more attention and more work.

Acknowledgements

This work is partly supported by AFOSR grant # FA9550-11-1-0176, NSF ARRA grant DMS 0908274, and by ERC Advanced Grant Project MULTIMOD-267184. The authors also thank the National Science Foundation and the National Security Agency for support to the Fall 2010 special semester on inverse problems at MSRI, Berkeley.

References

[1] H. Ammari, J. Garnier, H. Kang, W.-K. Park, and K. Sølna, Imaging schemes for perfectly conducting cracks, SIAM J. Appl. Math., 71 (2011), 68–91.

[2] H. Ammari, J. Garnier, and K. Sølna, A statistical approach to target detection and localization in the presence of noise, Waves in Random and Complex Media, 22 (2012), 40–65.

[3] H. Ammari and H. Kang, *Reconstruction of Small Inhomogeneities from Boundary Measurements*, Lecture Notes in Mathematics, Volume 1846, Springer-Verlag, Berlin, 2004.

[4] H. Ammari, M. Vogelius, and D. Volkov, Asymptotic formulas for perturbations in the electromagnetic fields due to the presence of inhomogeneities of small diameter II. The full Maxwell equations, J. Math. Pures Appl., 80 (2001), 769–814.

[5] H. Ammari and D. Volkov, The leading-order term in the asymptotic expansion of the scattering amplitude of a collection of finite number of dielectric inhomogeneities of small diameter, International Journal for Multiscale Computational Engineering, 3 (2005), 149–160.

[6] B. Angelsen, *Ultrasound Imaging. Waves, Signals and Signal Processing*, Emantec, Trondheim, 2000.

[7] A. Aubry and A. Derode, Random matrix theory applied to acoustic backscattering and imaging in complex media, Phys. Rev. Lett. 102 (2009), 084301.

[8] A. Aubry and A. Derode, Singular value distribution of the propagation matrix in random scattering media, Waves Random Complex Media 20 (2010), 333–363.

[9] A. Aubry and A. Derode, Detection and imaging in a random medium: A matrix method to overcome multiple scattering and aberration, J. Appl. Physics 106 (2009), 044903.

[10] J. Baik, G. Ben Arous, and S. Péché, Phase transition of the largest eigenvalue for nonnull complex sample covariance matrices, Ann. Probab., 33 (2005), 1643–1697.

[11] J. Baik, R. Buckingham, and J. DiFranco, Asymptotics of Tracy-Widom distributions and the total integral of a Painlevé II function, Communications in Mathematical Physics, 280 (2008), 463–497.

[12] J. Baik and J. W. Silverstein, Eigenvalues of large sample covariance matrices of spiked population models, Journal of Multivariate Analysis 97 (2006), 1382–1408.

[13] F. Benaych-Georges and R. R. Nadakuditi, The eigenvalues and eigenvectors of finite, low rank perturbations of large random matrices, Advances in Mathematics 227 (2011), 494–521.

[14] F. Bornemann, On the numerical evaluation of distributions in random matrix theory: a review, arXiv:0904.1581v5.

[15] M. Capitaine, C. Donati-Martin, and D. Féral, Central limit theorems for eigenvalues of deformations of Wigner matrices, Ann. Inst. H. Poincaré Probab. Statist., 48 (2012), 107-133.

[16] F. Chapon, R. Couillet, W. Hachem, and X. Mestre, The outliers among the singular values of large rectangular matrices with additive fixed rank deformation, arXiv:1207.0471.

[17] W. Elmore and M. Heald, *Physics of Waves*, Dover, New York, 1969.

[18] J.-P. Fouque, J. Garnier, G. Papanicolaou, and K. Sølna, *Wave Propagation and Time Reversal in Randomly Layered Media,* Springer, New York, 2007.

[19] J. Garnier and G. Papanicolaou, Resolution analysis for imaging with noise, Inverse Problems, 26 (2010), 074001.

[20] L. Györfi, I. Vajda, and E. Van Der Meulen, Minimum Kolmogorov distance estimates of parameters and parametrized distributions, Metrika, 43 (1996), 237–255.

[21] J. Hadamard, Résolution d'une question relative aux déterminants, Bull. Sci. Math., 17 (1893), 30–31.

[22] R. A. Horn and C. R. Johnson, *Matrix Analysis*, Cambridge University Press, Cambridge, 1985.

[23] I. M. Johnstone, On the distribution of the largest eigenvalue in principal components analysis, Ann. Statist., 29 (2001), 295–327.

[24] V. A. Marcenko and L. A. Pastur, Distributions of eigenvalues of some sets of random matrices, Math. USSR-Sb., 1 (1967), 507–536.

[25] A. Shabalin and A. Nobel, Reconstruction of a low-rank matrix in the presence of Gaussian noise, Journal of Multivariate Analysis, 118 (2013), 67–76.

[26] S. Stergiopoulos, *Advanced Signal Processing Handbook: Theory and Implementation for Radar, Sonar, and Medical Imaging real-time systems*, CRC Press LLC, Boca Raton, 2001.

[27] G. W. Stewart, Perturbation theory for the singular value decomposition, in *SVD and Signal Processing, II: Algorithms, Analysis and Applications*, Elsevier, 1990, pp. 99–109.